Inset-fed microstrip patch antenna optimization for 2.4 GHz using surrogate model assisted differential evolution machine learning algorithm

Magnoudewa Alaba[1], Dominic Bernard Onyango Konditi[2], Vitalice Kalecha Oduol[3]
[1]Department of Electrical Engineering (Telecommunication Option), Pan African University, Institute for Basic Sciences Technology and Innovation (PAUSTI), Nairobi, Kenya
[2]School of Electrical and Electronics Engineering, Technical University of Kenya (TUK), Nairobi, Kenya
[3]Department of Electrical and Information Engineering, Faculty of Engineering, University of Nairobi (UoN), Nairobi, Kenya

Article Info

Article history:

Received Mar 15, 2024
Revised Jun 25, 2024
Accepted Jul 20, 2024

Keywords:

ADE
Expanded bandwidth
Inset-fed patch
Parameter optimization
Performance metrics
SADEA

ABSTRACT

In this work, we have used the surrogate model assisted differential evolution (SADEA) to model a one and two-element inset-fed patch antenna array to optimize its parameters for efficiency and usability. The microstrip patch antennas operates in a frequency band of 2.4 GHz. The optimization process focused on fine-tuning the patch length, patch width, and notch width to enhance key performance metrics directivity, return loss, and bandwidth. The design is made in CST software with an FR-4 substrate and simulated in the ADE1.0 software a MATLAB toolbox. Significant enhancements were achieved including a directivity gain of 3.04 dB, and 5.58 dB a return loss of -19 dB, -16 dB, and an expanded impedance bandwidth from 0.0798 GHz, 0.0588 GHz to 0.0951 GHz, 0.0824 GHz respectively. The antenna was constructed and then measured. The findings showed that the measurements and the fabrication process closely matched, especially in terms of return loss.

Corresponding Author:

Magnoudewa Alaba
Department of Electrical Engineering (Telecommunication Option)
Pan African University, Institute for basic Science Technology and Innovation (PAUSTI)
Nairobi, Kenya
Email: alaba.magnoudewa@students.jkuat.ac.ke

1. INTRODUCTION

The ever-growing population and high demand for wireless communication systems require reliable and efficient data transfer communication where antenna play a key role [1]. To maximize the effectiveness of engineer's designs, optimization is typically required across all engineering specialties [2]. The fundamental microstrip patch antenna consists of a radiating patch, usually composed of conductive materials like copper or gold, on one side of a dielectric substrate and a ground plane on the other [3]. The 2.4 GHz frequency band is widely used in internet of things (IoT) due to its compatibility with existing technologies, versatile range, cost-effectiveness, and global standardization [4]. Although optimization can improve the performance of antennas, conventional techniques are computationally costly [5]. The development of surrogate model-assisted differential evolution for antenna synthesis (SADEA) offers a significant improvement in efficiency over conventional methods to tackle this issue [6]. SADEA optimizes antenna designs efficiently by combining differential evolution (DE) with surrogate modeling, which is especially useful for intricate systems. Antenna design explorer (ADE) is a tool designed to help antenna engineers explore designs more effectively with SADEA by giving priority to functionality, generality, and usability [7].

The optimization of a rectangular inset-fed patch microstrip antenna for IoT applications using the (SADEA) algorithm is proposed.

Singh and Tripathi [8] conducted a survey on microstrip patch antennas, highlighting their advantages over conventional microwave antennas like reduced weight, volume, and cost. They explored different types, feeding techniques, and applications, comparing them to traditional microwave antennas. The survey also explored array configurations to address drawbacks like low gain or limited power handling capacity. Overall, the survey provided a comprehensive overview of microstrip patch antennas. Khaliluzzaman *et al.* [9] have developed a new H-shaped wideband microstrip patch antenna for wireless local area network (WLAN) applications at 4 GHz. The antenna, made of Rogers RT-5880 substrate, features a rectangular patch with dimensions of 29.6 mm width and 24.5 mm length. The antenna's performance was enhanced by incorporating a pair of slits along a radiating edge, resulting in superior bandwidth and multiple resonant frequencies. This antenna holds potential for widespread WLAN applications. Sinha *et al.* [10] developed a 2×2 rectangular microstrip phased array antenna for global system for mobile communication (GSM) applications. The design, tested using a high-frequency structure simulator (HFSS) simulator on a 1.5 cm thick RT Duroid substrate, achieved superior performance at 900 MHz center frequency. Simulated results showed gain values averaging 13-14 dBi, ideal for GSM applications. The antenna's efficacy was confirmed through measured and simulated data for resonant frequency, return loss, and radiation patterns.

The study by Vijayalakshmi and Rubasri [11] focused on designing and simulating microstrip circular patch antenna arrays using edge feeding techniques for WLAN applications on the 2.4 GHz frequency range. The antennas were made with FR-4 Epoxy Glass Substrate for improved performance. The HFSS software tool was used to simulate the arrays and evaluate parameters like gain, return loss, radiation pattern, and voltage standing wave ratio (VSWR) at high frequencies, and an 8×8 multiple-input multiple-output (MIMO) antenna array was developed, capable of transmitting signals up to -20 dBm within 62 mm space and providing a 5 dB gain over the frequency range of 2.40 GHz to 2.5 GHz. The researchers's study focused on designing microstrip patch antennas using an artificial neural network (ANN) model in [12]. Their innovative approach involved in reduce ground size to achieve an ultrawideband frequency range, a technique that outperforms traditional electromagnetic simulation software. The method extracts crucial parameters for antenna design at specific frequencies, eliminating the need for iterative procedures or expensive software packages. The study compares the ANN results with experimental data, finding the radial basis function network for its accuracy and speed in implementing the proposed antenna design.

Dundar *et al.* [13] investigated the use of artificial intelligence (AI) in designing and optimizing microstrip antennas. It used data from 144 simulations using Hyper-Lynx® 3D EM electromagnetic simulator and two machine learning models: the multilayer perceptron (MLP) and the K-nearest neighbors algorithm model. The firefly algorithm is used for optimization, enabling simulation of the antenna model using CST Studio Suite 2011 software. The research highlights the potential of AI in improving microstrip antenna design and optimization processes. Gouda and Mehta [14] explored software cost estimation in early stages of software development by introducing novel adaptive mutation operators, including a syndrome adaptive mutation operator, to enhance solution diversity. They used meta-heuristic algorithms to optimize mathematical and software models, offering solutions for accurately predicting software parameters. Comparative analyses show superior mutation results compared to standard algorithms, demonstrating enhanced predictive capabilities for cost estimation and potential for accurate software parameter forecasting. A self-adaptive collaborative differential evolution algorithm (SADEA) to solve the ERM problem under uncertainty was proposed in [15]. SADEA uses a three-stage adaptive collaboration strategy, including boundary randomization, knowledge-assisted collaboration, and range restructuration, to generate collaborative solutions. Different DE strategies are selected based on count values and random factors. The algorithm's legitimacy and robustness are ensured through boundary control, elite selection, and retention. Compared to other algorithms, SADEA outperforms them in objective function, ranking index, and convergence, making it effective in handling uncertainty.

The researchers presented a method for optimizing human activity recognition (HAR) using a SADEA-I [16]. The approach refined signal processing, adaptive thresholding, and classification parameters, resulting in accuracies of 89.41% and 93.54%, respectively. The method was evaluated with support vector machine (SVM) and AlexNet, highlighting its performance improvements, and also offered advantages like contactless operation and privacy preservation. The method showed significant accuracy enhancements compared to manually tuned systems, with SADEA-I optimization leading to substantial reductions in error rates. The study in [17], focused on optimizing a bowtie-dipole antenna for through-the-wall imaging using a hybrid approach that combined finite difference time domain and method of moment's computational electromagnetic techniques. The antenna shapes were parameterized using the SADEA, which integrates the capabilities of a CST microwave studio electromagnetic design environment with MATLAB computing and programming. The compact ultra-wideband antenna, measuring 12.87 mm×28.62 mm, is achieved with optimal parameters. The author introduced the DE algorithm, renowned for its high resolution and optimization speed in continuous spaces. A solution for optimizing antenna designs in commercial electromagnetic simulation software known as ADE was introduced. It incorporates advanced antenna design exploration methods, efficient optimization, and multi-objective optimization. ADE offers usability features, automatic parameter setting, and interactive stopping criteria. It is compatible with existing simulators and optimizers [18].

The literature review highlights the potential of SADEA in improving antenna designs, but there is limited research on optimizing SADEA for high gain, return loss and other parameters in patch array antennas, particularly for IoT applications. The paper explores the optimization of an antenna operating at 2.4 GHz using the SADEA algorithm. To improve important performance parameters including directivity gain, return loss, and bandwidth, the optimization method concentrated on adjusting several parameters, including the length and width. Additionally, the study emphasized the significance of effective antenna design in reducing propagation losses in IoT technologies, as well as the crucial role optimization techniques play in communication systems. The expanding importance of MATLAB in communication engineering is reflected in the paper's discussion of the usefulness of ADE software, a MATLAB toolbox, and the CST suite for antenna design and simulation. Additionally, the DE algorithm is introduced, renowned for its effectiveness in antenna design and analysis, offering high resolution and optimization speed in continuous spaces. In summary, the paper demonstrates the efficacy of the SADEA algorithm in optimizing microstrip antenna performance, underscoring the significance of efficient antenna design in addressing the challenges posed by IoT technology. This study focuses on creating one and two microstrip patch antennas using CST Studio, then simulating the results using ADE software to optimize the CST software original design. The structure of the paper is as follows: the literature review is covered in the second section, the methodology is described in the third, the results are presented and discussed in the fourth, and concluding in the final section.

2. METHOD

The proposed antenna design methodology involves conceptualizing, creating, optimizing, and fabricating the final design. Initial design considerations include selecting the antenna type, determining parameters, and applying optimization techniques. The antenna is then fabricated using appropriate techniques and materials for consistency and reliability.

2.1. Antenna design and dimension

In the realm of antenna engineering, the microstrip patch antenna is ingeniously depicted within the "Transmission Line model". Here, in Figure 1 the antenna materializes as a purposeful conductor with defined dimensions a width denoted as 'W,' a height specified as 'h,' and a distinct length identified as 'L', as shown in Figure 1(a). Notably, the antenna's height 'h' is intricately calibrated within the nuanced range of 0.333 λ_0 to 0.5 λ_0 as Figure 1(b) illustrate. Adding a layer of sophistication, the substrate, often fashioned from FR-4, contributes to the antenna's overall performance, emphasizing a seamless fusion of material science and electromagnetic precision. Figure 1(c) is the fabricated view of the single microstrip antenna. Figure 2 shows the perspective, front, and fabricated view of the two elements. Figure 2(a) reveals the perspective view and the layer of the antenna while Figure 2(b) shows the front view. The effective functioning of a microstrip antenna is intricately tied to its dimensions as shown in Figure 1, which are determined by established design equations. These equations act as essential guides, enabling the calculation of specific patch dimensions critical for achieving optimal antenna performance. They offer a systematic framework for arriving at the necessary dimensions, ensuring the antenna meets the desired performance criteria. Figure 2(c) is the fabricated view of the double-patch microstrip antenna.

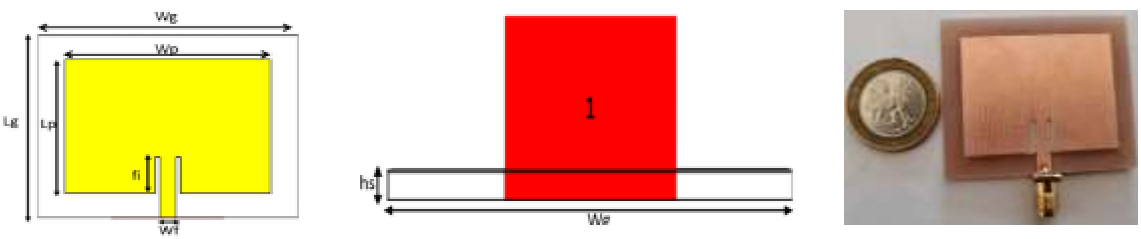

(a) (b) (c)

Figure 1. Single proposed MPA view layout in CST microwave: (a) front, (b) bottom, and (c) measured

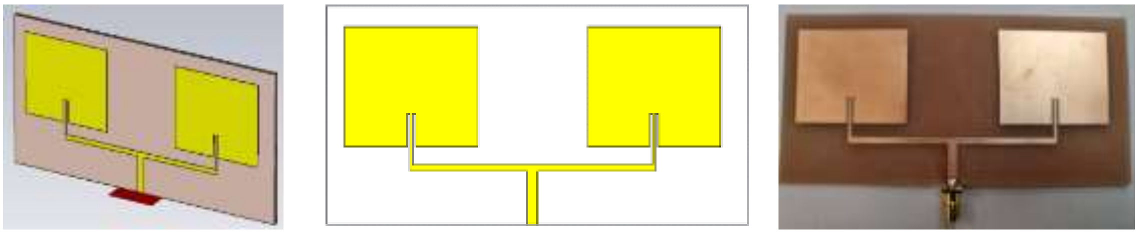

(a) (b) (c)

Figure 2. MPA array 1×2 or double view layout in CST microwave: (a) perspective, (b) front, and (c) measured

Design steps are as follows: effective dielectric constant, ε_{rff} Using the formula by [19], [20] The relative effective permittivity is calculated from the value obtained from (1).

$$\varepsilon_{reff} = \frac{(\varepsilon_r + 1)}{2} + \frac{(\varepsilon_r - 1)}{2}\left[1 + 12\frac{h}{w}\right]^{-\frac{1}{2}} \quad (1)$$

Where h is the thickness of the substrate in mm, Wp is the width of the patch in mm. The patch width,

$$W = \frac{c}{2f\sqrt{\frac{\varepsilon_R + 1}{2}}} \quad (2)$$

Effective length, L_{eff},

$$Lp = \frac{c}{2f\sqrt{\varepsilon_{Reff}}} \quad L_{eff} = L + 2\Delta L \; \Delta L = 0.412h\left(\frac{\varepsilon_{Reff} + 0.3}{\varepsilon_{Reff} - 0.258}\right) + \frac{\frac{w(i)}{h} + 0.264}{\frac{W(i)}{h} - 0.258} \quad (3)$$

Where, Lp=length of patch, εeff=effective substrate, Wp=width of patch+ΔL=fringing field of the antenna Ground dimensions,

$$Lg = 6h + Lp \;\; Wg = 6h + Wp \quad (4)$$

where Wg and Lg are the ground plane's width and length, respectively, in millimeters.

The antenna parameters outlined in this study are computed and simulated using CST Microwave Studio. The substrate employed is FR-4, characterized by a relative permittivity of 4.3. The schematic of the microstrip antenna design is illustrated in Figures 1 and 2. The antenna dimensions are outlined in a Table 1.

Table 1. Antenna parameters and dimension

Parameter	Dimension (mm)
Frequency	2.4 GHz
Ground Length, L_g	39
Ground Width, W_g	48
Length of the patch L_p	29
width of the patch W_p	38
Height of substrate	1.6
Dielectric Constant	4.3
Feedline insertion, f_i	1.6
Loss Tangent	0.025
Width of feedline, W_f	3.13
Ground Thickness, H_t	0.035

2.2. Optimization of antenna using the SADEA algorithm

SADEA integrates the DE algorithm for parameter optimization and the gaussian process (GP) model for performance prediction, effectively reducing computational costs and accelerating convergence in complex tasks such as antenna synthesis. In the following sub-section, the GP process and the DE algorithm are explained. The ADE used for the SADEA optimization is underlined with their architectures.

2.2.1. Gaussian process

In GP, the objective function follows a GP. It predicts new point values and uncertainty based on existing data, aiding in candidate selection for evaluations. Assume we possess n training data $x = (x_{1,}\ x_{2,} \dots \dots x_k)$ with associated exact function values $y = (y_{1,} y_2 \dots \dots . y_k)$. Employing the GP model alongside the correlation function $C(x_{i,} x_{j,})$, we can forecast the function value $y(x^{\tau})$ at a new point x^{τ} as follows [21]:

$$\hat{y}(x^{\tau}) = \mu + r^T Z^{-1}(y - I\mu) \tag{5}$$

where,
$\hat{\mu} = (I^T Z^{-1} I)^{-1} I^T Z^{-1} y$
$Z_{i,j} = C(x_{i\,,} x_j), i, j = 1,2, \dots . , k$

$$r = [C(x^{\tau}, x_1), C(x^{\tau}, x_2), \dots . . C(x^{\tau}, x_n)] \tag{6}$$

In (7) provides an illustration of a correlation function.

$$C(x_1 x_2) = exp\left(-\sum_{\gamma=1}^{d} \theta_\gamma \left|x_i^\gamma - x_j^\gamma\right| p_\gamma\right)\ \ \theta_\gamma > 0,1 \le p_\gamma \le 2 \tag{7}$$

Here, θ_γ is the correlation parameter controlling correlation decrease, and x_i^γ relates to function smoothness, with x^γ being associated. where d denotes dimension of *x*. The parameters θ_γ and p_γ are determined by GP maximizing the likelihood function.

$$m = \frac{1}{(2\pi)^{n/2} (\sigma^2)^{n/2} |Z|^{1/2}} exp\left(-\frac{(y - I_\mu)^T Z^{-1}(y - I\mu)}{2\sigma^2}\right) \tag{8}$$

Here, I denote a vector of ones. where θ_γ *and* p_γ are given by setting the derivatives of the likelihood function to zero, μ becomes $\hat{\mu}$ derived from (6), and σ^2 is be computed.

$$\hat{\sigma}^2 = (y - I\hat{\mu})^T Z^{-1}(y - I\hat{\mu}) n - 1 \tag{9}$$

By replacing $\hat{\mu}$ and $\hat{\sigma}^2$ in (8) it maximized it to obtain an estimated of $\hat{\theta}_\gamma$ and $\hat{p}_\gamma$.

$$\hat{s}^2(x^{\tau}) = \hat{\sigma}^2 [I - r^T Z^{-1} + (I - r^T Z^{-1} r)^2 (I^T Z^{-1} I)^{-1}] \tag{10}$$

The prescreening methods is used to measure the candidate design using (5) and (10). The introduction of the lower confidence bound (LCB) prescreening that is used in SADEA given a problem minimization.

$$y_{lcb}(x) = \hat{y} - w\hat{s}(x) \tag{11}$$

W being a constant, which is to (2). In [18], [22] there is explanation that can be found.

2.2.2. Differential evolution

DE [22] is a widely used population-based metaheuristic algorithm for continuous optimization, incorporated into SADEA. Several DE mutation strategies exist, each offering different trade-offs between convergence rate and population diversity. The characteristics of various DE mutation strategies within the SADEA framework have been examined in [22]. A few information will be presented.

Let S the population and best element in S is x^{best}, where $x = (x_{1,\dots\dots} x_d)$ is an element solution in S. For child solution generation $u = (u_{1,\dots\dots,} u_d)$ for x. Mutation: DE/current-to-best/1 and DE/best/1.

$$y^i = x^i + F(x^{best} - x^i) + F(x^{r1} - x^{r2})\ \ y^i = x^{best} + F(x^{r1} - x^{r2}) \tag{12}$$

F being the constant ranging (0,2], x^i an element of S where x^{r1} *and* x^{r2} are two random solution chose from S but not the same as x^{best}. y^i is the donor vector after mutation.

Crossover: child production n as follows: let select a variable index k_{rand} is set as $\in \{1, \dots . . , d\}$ where when $k = 1$ to d generate random numbers in the range [0,1].

$$n_{i,j} = \begin{cases} y_{ij}, & if\ (rand \leq CR) J = k_{rand} \\ x_{i,j}, & otherwise \end{cases} \quad (13)$$

CR is the crossover rate in the range of [0,1]. In [21] details can be found for more explanation.

In order to improve the return loss and increase the gain we adjusted the antenna using the SADEA technique, described in [23], using the ADE optimization tool. The algorithm that optimizes the antenna's performance is shown graphically in Figure 3. The SADEA algorithm comprises 7 steps for antenna design exploration. In the final stage, promising child solutions undergo electromagnetic (EM) simulations and are included in the database for iterative refinement [24], [25]. The DE/best/1 mutation strategy, employed in DE algorithms, aims to generate new candidate solutions by perturbing the best solution found so far (denoted as "best") and two randomly selected solutions from the current population. The mutation operation, defined as in (12) involves parameters such as y^i for the new candidate solution, x^{best} for the best solution, x^{r1} and x^{r2} for randomly selected solutions, and F as the scaling factor controlling the perturbation magnitude. Following mutation, the crossover operation combines candidate and parent solutions to generate the final child solution. In the DE/best/1 mutation strategy, binomial crossover, a stochastic operation, is typically used, randomly selecting elements from both the candidate and parent solutions [24].

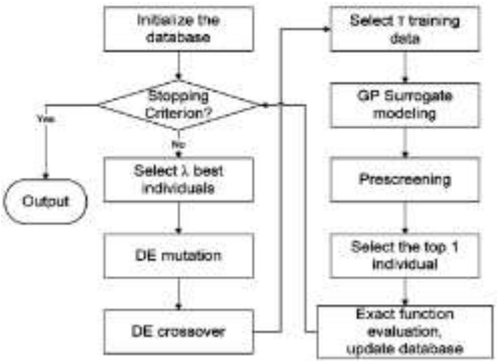

Figure 3. Flow diagram of SADEA optimization

2.3. Antenna design explorer

ADE is MATLAB's Toolbox that provides a complete environment for designing and optimizing antennas, enabling engineers and researchers to create antenna structures that meet specific performance criteria. It is a powerful tool that can save time and improve the accuracy of antenna design and optimization compared to traditional methods this technique has been well explained in [18]. Figure 4 shows the working layout of the ADE. Figure 4(a) shows the architecture and Figure 4(b) the start window of the ADE respectively.

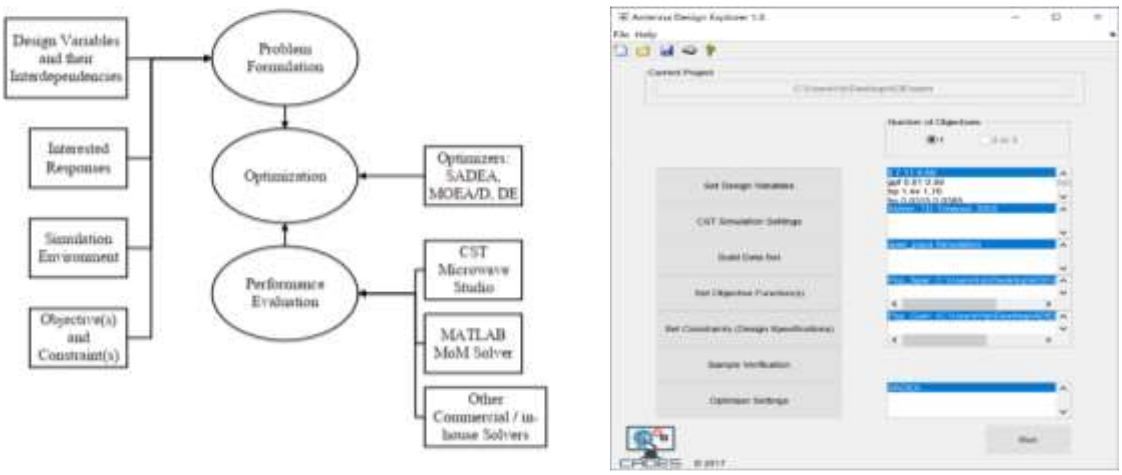

(a) (b)

Figure 4. Architecture and start window (a) ADE architecture [7] and (b) ADE starting window

The algorithm explanation comprises the following phases [18]:
A- Design variable setup with respective ranges.
B- Imposition of geometrical constraints, addressed efficiently without costly EM simulations using ADE.
C- Specification of simulation settings for CST Microwave Studio, including installation path, solver type, and estimated simulation time.
D- Creation of a dataset, specifying desired responses for optimization, either through CST simulation or other EM tools like MATLAB.
E- Establishment of objective function(s) based on selected responses, facilitated by an m-file template.
F- Setting constraints based on identified responses, also using an m-file template.
G- Validation of objective and constraint functions for a single design, and exploration of the design landscape through sample verification.
H- Selection of optimization algorithms and parameter setup, including embedded optimizers or custom algorithms for antenna design exploration

3. RESULTS AND DISCUSSION

This section provides an overview of the outcomes and analyses of the design and experiment. The discussion of the findings starts with the examination of the system's performance and the ADE optimization, including the results of return loss (expressed in decibels), VSWR, and far-field gain. This is accomplished by using the CST Studio software in conjunction with the ADE1.0 MATLAB toolbox.

3.1. The system evaluation performance

The design, modeling, and simulation of single and double microstrip patch antennas in CST Studio, optimized with SADEA in ADE 1.0, yield substantial enhancements. Initial CST results at 2.4 GHz exhibit return loss S11 values of -17.95 dB and -9.73 dB, with gains of 2.60 dB and 4.6 dB for single and double patch antennas, respectively. Following optimization with SADEA, S11 values improve to -19.89 dB and -16.09 dB, with gains reaching 3.04 dB and 5.58 dB, respectively. Fabrication validates the design's effectiveness, although slight deviations in resonance frequencies between simulation and measurement arise, primarily due to cable and SMA plug losses affecting the S11 shift. Despite these discrepancies, all S11 values remain below -10 dB, affirming satisfactory performance. Illustrated in Figures 5 and 6 is the optimization graph where Figures 7 to 9 are simulated results for S11, VSWR, and gain, respectively, with a comprehensive summary provided in Figure 10 and Table 2. Additionally, Table 3 offers a comparative analysis with other studies, emphasizing the efficacy of the proposed antenna design.

3.2. The optimization in ADE 1.0

When analyzing optimization results, two key factors are crucial: population diversity and convergence trends. Population diversity, as measured by the standard deviation among individuals, indicates the range of solutions explored. Low diversity suggests a limited potential for improvement, as shown in Figure 5(a) with a value of 0.659 and Figure 5(b) with a value of 0.338. The convergence trend, observed through ADE 1.0, shows the best solution's performance over iterations. In the provided test case in Figure 6(a), significant progress is evident after 230 simulated iterations, with clear convergence and minimal diversity around 500 simulated iterations, whereas Figure 6(b) also reaches its peak at 230 simulated iterations, with clear convergence and minimal diversity around 350 simulated iterations, signaling the end of optimization of the single and double elements, respectively. It also shows the dialogue on how the optimization can continue and the result of the optimization.

3.3. Return loss

Return loss in RF systems measures power transfer efficiency, with a baseline of -10 dB indicating minimal signal loss and optimal power utilization for mobile communication. Figure 7(a) shows the return loss of the single element (SE) with a value of -17.95 dB, and Figure 7(b) illustrates the return loss of the double element (DE) with a value of -9.73 dB, both designed in CST. After the optimization, Figure 7(c) shows a value of -19.89 dB for the optimized single element (SEOP), and Figure 7(d) shows a value of -16.09 dB for the double element optimization (DEOP), which proves the improvement of the result from Figures 7(a) to 7(c) and Figure 7(b) to 7(d). The MPA array resonates at 2.4 GHz, as shown in Figure 7. The measured antennas are shown in Figure 7(e) to 7(h). From the single measured (SEM) in Figure 7(e), the double measured (DEM) in Figure 7(f), and the optimized measure in Figures 7(g) and 7(h) for single (SEOPM) and double (DEOPM), respectively, the measure figures show a slight shifting in the frequency range.

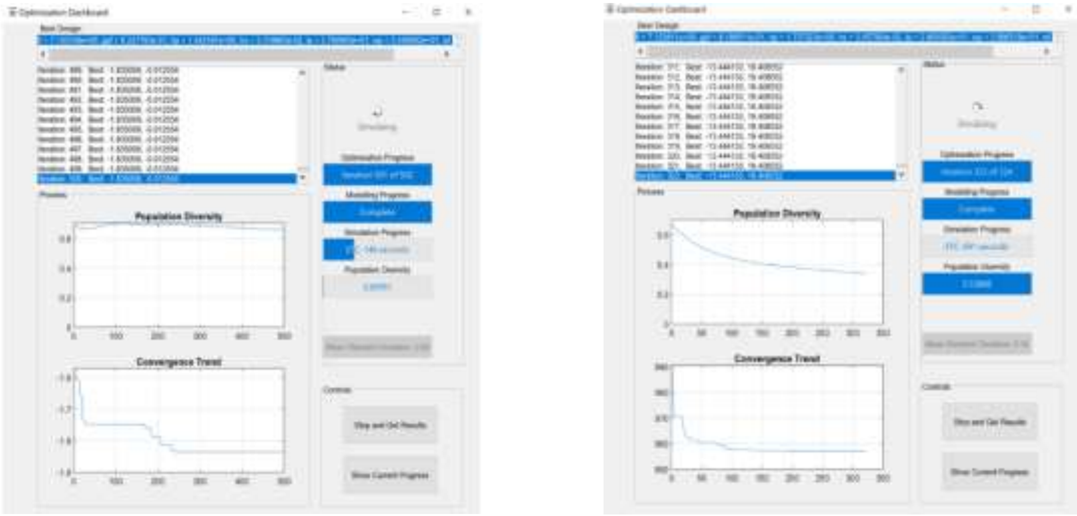

(a) (b)

Figure 5. Optimization monitoring process for each element (a) single and (b) double

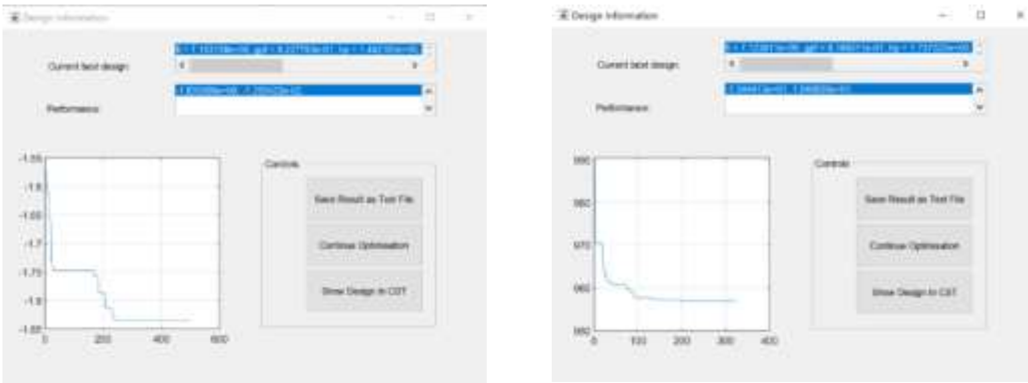

(a) (b)

Figure 6. The optimization dialogue box for each element (a) single and (b) double

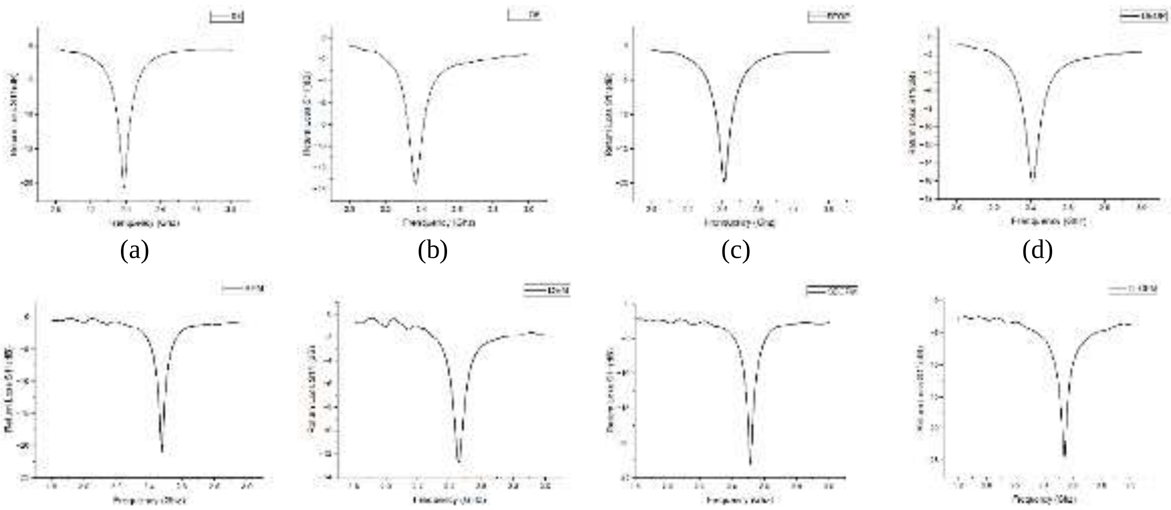

(a) (b) (c) (d)

(e) (f) (g) (h)

Figure 7. Return loss over the suggested antenna's frequency: (a) single CST, (b) double CST, (c) single optimized, (d) double optimized, (e) single CST measured, (f) double CST measured, (g) single optimized measured, and (h) single optimized measured

3.4. Voltage standing wave ratio

Patch antennas should maintain a VSWR below 2 for efficient power transfer and minimal signal reflection, optimizing performance in communication systems. Figure 8(a) shows the VSWR result for the SE, with a value of 1.29 and a value of 1.96 for the DE in Figure 8(b). The optimized VSWR result is illustrated in Figure 8(c) and 8(d), where single element (SEOP) and double element (DEOP) have values of 1.22 and 1.37, respectively, to show the improvement after the optimization is done.

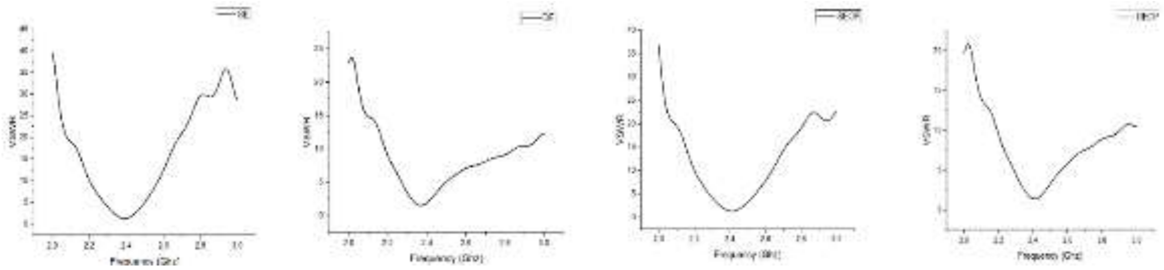

(a) (b) (c) (d)

Figure 8. VSWR (a) single CST, (b) double CST, (c) single optimized, and (d) double optimized

3.5. Far-field gain

Gain in antennas measures the efficiency of converting input power into radio waves, with higher gain indicating stronger radiation concentration, enhancing signal strength and coverage. The SE and DE simulated in CST are shown in Figures 9(a) and 9(d) with a value of 2.60 dB and 4.61 dB, respectively, showing the 3-D radiation pattern of antennas. The optimized element is shown in Figures 9(b) and 9(e) with a value of 3.04 dB and 5.58 dB, respectively. The polar radiation pattern of the antenna is shown in Figures 9(c) and 9(f).

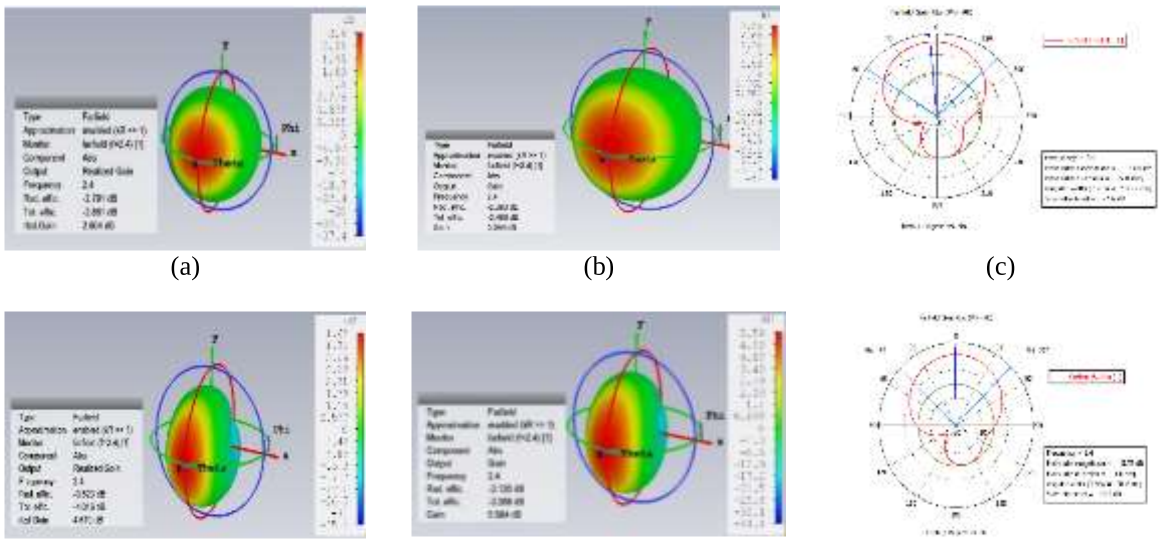

(a) (b) (c)

(d) (e) (f)

Figure 9. Gain (a) single in CST, (b) single optimized, (c) single polar form (d) double in CST, (e) double optimized, and (f) double polar form

3.6. Summary of result

The summary of the simulated and measured results displays the comparisons of return loss values, the VSWR, the far-field gain, and the directivity for single and double elements, respectively, as shown in Figure 10 and Table 2. Figure 10(a) illustrates the return loss of all the single elements, and Figure 10(b) shows the double element, while Figure 10(c) shows both elements VSWR.

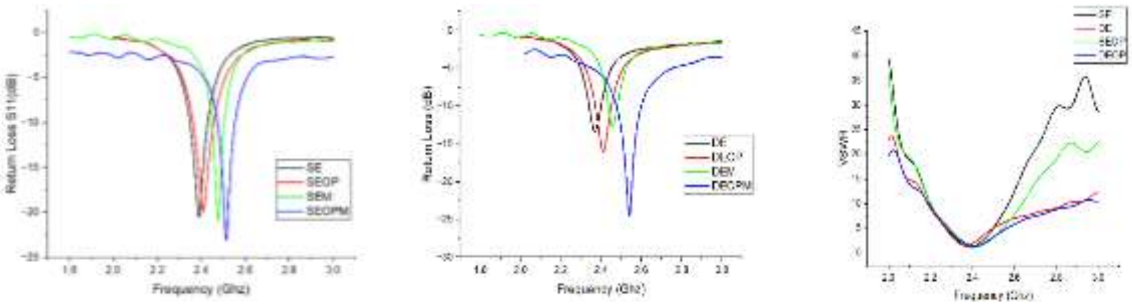

(a) (b) (c)

Figure 10. Summarise of the result (a) return loss for single, (b) return loss for double, and (c) VSWR for both

Table 2. The performance of the antenna in CST and the optimization using SADEA

Antenna parameters	In CST		Optimization in ADE using SADEA	
Element	Single	Two	Single	Two
Return loss (dB)	-17.95	-9.73	-19.89	-16.09
VSWR	1.29	1.96	1.22	1.37
Realized gain (dB)	2.60	4.6	3.04	5.58
Directivity	5.46	8.63	5.61	8.71

3.7. Performance comparison

A microstrip 2.4 GHz antenna is the suggested antenna. Researchers displayed a number of antennas with similar topologies and frequencies, along with experimental and parametric data for a range of uses. As the comparison shows, the suggested rectangular antenna performs better than all other designs, as indicated by the Table 3. The suggested antenna also performs better at 2.4 GHz than other options, making it a practical choice for 2.4 GHz IoT applications.

Table 3. Comparison with others works

Year	Ref.	Antenna shape and method	Antenna size	Gain (dB)	Return loss	VSWR	Directivity (dB)	Bandwidth (Ghz)	Application
2017	[26]	Spiral slot / impedance matching circuit design for dual-band antenna	12.45×13.05	1.06	<-10	-	1.62	-	-
2020	[27]	Slotted SIW array antenna design"	120.0×395.4	4.80	-	-	-	-	WLAN
2021	[28]	Rectangular / parameter tuning.	26.00×19.00	5.05	-12.54	1.6	-	0.0665	IoT
2022	[29]	Rectangular / simulation using CST	20.00×15.00	1.39	-2.12	-	-	-	IoT
2023	[30]	L-shaped / parameter tuning	28.00×21.00	2.09	-	-	-	-	IoT
2024	This paper	Rectangular / SADEA algorithm	39.00×29.00	5.58	-16.09	1.37	8.71	0.0809	IoT

4. CONCLUSION

This study focuses on the design and simulation of a one and two-element inset-fed microstrip patch antenna, operating at a center frequency of 2.4 GHz, using CST Studio software. The antennas underwent optimization using the SADEA algorithm within ADE. Various parameters were adjusted during optimization. The results indicate significant improvements in return loss (-19.89 dB and -16.09 dB) and gains (3.04 dB and 5.58 dB), as well as an expanded impedance bandwidth of 0.0809 GHz. The proposed antenna after the successful simulation and optimization was fabricated to validate the design effectiveness. While the study emphasized software-based simulations and fabrication, it suggests future research avenues exploring the design and practical performance of differently shaped patch antennas.

ACKNOWLEDGEMENTS

The authors extend their gratitude to the African Union Commission for their financial contribution and to the members of the Pan African University Institute for Basic Sciences, Technology, and Innovation. We further extend our appreciation to Dr Jeremiah Abolade for his tremendous guidance and support.

REFERENCES

[1] D. A. J. Al-Khaffaf and I. A. Alshimaysawe, "Miniaturised tri-band microstrip patch antenna design for radio and millimetre waves of 5G devices," *Indonesian Journal of Electrical Engineering and Computer Science (IJEECS)*, vol. 21, no. 3, pp. 1594–1601, Mar. 2021, doi: 10.11591/ijeecs.v21.i3.pp1594-1601.

[2] B. Manoj and S. Rodriguez, "Optimization of microstrip patch antenna dimensions for enhanced bandwidth, operating frequency, return loss and feed width using genetic algorithm," in *2021 7th International Conference on Advanced Computing and Communication Systems (ICACCS)*, Mar. 2021, pp. 598–603, doi: 10.1109/ICACCS51430.2021.9441673.

[3] M. R. Hire and C. S. Ahire, "A review on microstrip patch antenna design and its applications," *SSRN Electronic Journal*, 2022, doi: 10.2139/ssrn.4043696.

[4] A. M. Abdulhussein, A. H. Khidhir, and A. A. Naser, "2.4 GHz microstrip patch antenna for S-band wireless communications," *Journal of Physics: Conference Series*, vol. 2114, no. 1, p. 012029, Dec. 2021, doi: 10.1088/1742-6596/2114/1/012029.

[5] M. O. Akinsolu, K. K. Mistry, B. Liu, P. I. Lazaridis, and P. Excell, "Machine learning-assisted antenna design optimization: a review and the state-of-the-art," in *2020 14th European Conference on Antennas and Propagation (EuCAP)*, Mar. 2020, pp. 1–5, doi: 10.23919/EuCAP48036.2020.9135936.

[6] S. Henthorn, M. O. Akinsolu, K. Lee Ford, B. Liu, and T. O'Farrell, "Machine learning-assisted optimization of a metasurface-based directly modulating antenna," in *2022 IEEE International Symposium on Antennas and Propagation and USNC-URSI Radio Science Meeting (AP-S/URSI)*, Jul. 2022, pp. 1888–1889, doi: 10.1109/AP-S/USNC-URSI47032.2022.9886083.

[7] B. Liu, A. Irvine, M. O. Akinsolu, O. Arabi, V. Grout, and N. Ali, "GUI design exploration software for microwave antennas," *Journal of Computational Design and Engineering*, vol. 4, no. 4, pp. 274–281, Oct. 2017, doi: 10.1016/j.jcde.2017.04.001.

[8] I. Singh and V. S. Tripathi, "Micro strip patch antenna and its applications : a survey," *International Journal of Computer Technology and Applications*, vol. 2, no. 5, pp. 1595–1599, 2011.

[9] M. Khaliluzzaman, D. kumar Chy, and M. R. H. Chowdhury, "Enhancing the bandwidth of a microstrip patch antenna at 4 GHz for WLAN using H-shaped patch," *IJISET-International Journal of Innovative Science, Engineering & Technology*, vol. 2, no. 2, 2015, [Online]. Available: www.ijiset.com.

[10] S. P. Sinha, M. Kumar, and J. Gupta, "Design of 2x2 shaped rectangular microstrip array antenna for GSM application," *International Journal of Scientific & Engineering Research*, vol. 6, no. 5, 20156.

[11] J. Vijayalakshmi, V. Dinesh, and S. Rubasri, "Design and analysis of high gain 2x1, 4x1, 8x1 and 8x8 circular patch antenna arrays for 2.4ghz applications," *International Journal of Scientific and Technology Research*, vol. 9, no. 4, pp. 834–841, 2020.

[12] S. Kaur, R. Khanna, P. Sahni, and N. Kumar, "Design and optimization of microstrip patch antenna using artificial neural networks," *International Journal of Innovative Technology and Exploring Engineering*, vol. 8, no. 9 Special Issue, pp. 611–616, Aug. 2019, doi: 10.35940/ijitee.I1097.0789S19.

[13] O. Dundar, E. Yelken, and S. Kocer, "Artificial intelligence methods used in microstrip antennas," *Current Studies in Artificial Intelligence, Virtual Reality and Augmented Reality*, pp. 146–162, 2022.

[14] S. K. Gouda and A. K. Mehta, "A self-adaptive differential evolution using a new adaption based operator for software cost estimation," *Journal of The Institution of Engineers (India): Series B*, vol. 104, no. 1, pp. 23–42, Feb. 2023, doi: 10.1007/s40031-022-00801-y.

[15] H. Qin, W. Bai, Y. Xiang, F. Liu, Y. Han, and L. Wang, "A self-adaptive collaborative differential evolution algorithm for solving energy resource management problems in smart grids," *IEEE Transactions on Evolutionary Computation*, pp. 1–1, 2024, doi: 10.1109/TEVC.2023.3312769.

[16] Z. Li, Y. Liu, B. Liu, J. Le Kernec, and S. Yang, "A holistic human activity recognition optimisation using AI techniques," *IET Radar, Sonar and Navigation*, vol. 18, no. 2, pp. 256–265, Sep. 2024, doi: 10.1049/rsn2.12474.

[17] R. Picking, "Institute of Electrical and Electronics Engineers United Kingdom and Republic of Ireland Section, Institute of Electrical and Electronics Engineers," 2017.

[18] M. O. Akinsolu *et al.*, "Antenna design explorer: A GUI software tool for efficient antenna design optimization," *IET Conference Publications*, vol. 2017, no. CP732, 2017, doi: 10.1049/cp.2017.0278.

[19] Interference Technology, "International Conference on Numerical Electromagnetic Modeling and Optimization for RF, Microwave and Terahertz Applications (NEMO) 2014," 2014.

[20] Y. Huang and K. Boyle, *Antennas: from theory to practice*. Wiley, 2008.

[21] B. Liu, S. Koziel, and N. Ali, "SADEA-II: a generalized method for efficient global optimization of antenna design," *Journal of Computational Design and Engineering*, vol. 4, no. 2, pp. 86–97, Apr. 2017, doi: 10.1016/j.jcde.2016.11.002.

[22] X. Tan and S. Y. Shin, "Differential evolution algorithm of soft island model based on K-means clustering," *Indonesian Journal of Electrical Engineering and Computer Science (IJEECS)*, vol. 19, no. 3, pp. 1548–1555, Sep. 2020, doi: 10.11591/ijeecs.v19.i3.pp1548-1555.

[23] B. Liu, H. Aliakbarian, Z. Ma, G. A. E. Vandenbosch, G. Gielen, and P. Excell, "An efficient method for antenna design optimization based on evolutionary computation and machine learning techniques," *IEEE Transactions on Antennas and Propagation*, vol. 62, no. 1, pp. 7–18, Jan. 2014, doi: 10.1109/TAP.2013.2283605.

[24] B. Liu, Q. Zhang, and G. G. E. Gielen, "A gaussian process surrogate model assisted evolutionary algorithm for medium scale expensive optimization problems," *IEEE Transactions on Evolutionary Computation*, vol. 18, no. 2, pp. 180–192, Apr. 2014, doi: 10.1109/TEVC.2013.2248012.

[25] B. Liu, M. O. Akinsolu, N. Ali, and R. Abd-Alhameed, "Efficient global optimisation of microwave antennas based on a parallel surrogate model-assisted evolutionary algorithm," *IET Microwaves, Antennas & Propagation*, vol. 13, no. 2, pp. 149–155, Feb. 2019, doi: 10.1049/iet-map.2018.5009.

[26] W. Liu, L. Xu, and H. Zhan, "Design of 2.4 GHz/5 GHz planar dual-band electrically small slot antenna based on impedance matching circuit," *AEU - International Journal of Electronics and Communications*, vol. 83, pp. 322–328, Jan. 2018, doi: 10.1016/j.aeue.2017.08.040.

[27] A. Izzuddin, A. Dewantari, E. Setijadi, E. Palantei, E. T. Rahardjo, and A. Munir, "Design of 2.4 GHz slotted SIW array antenna for WLAN application," in *2020 International Conference on Radar, Antenna, Microwave, Electronics, and Telecommunications (ICRAMET)*, Nov. 2020, pp. 70–73, doi: 10.1109/ICRAMET51080.2020.9298646.
[28] A. Irfansyah, B. B. Harianto, and N. Pambudiyatno, "Design of rectangular microstrip antenna 1x2 array for 5G communication," *Journal of Physics: Conference Series*, vol. 2117, no. 1, p. 012028, Nov. 2021, doi: 10.1088/1742-6596/2117/1/012028.
[29] A. J. A. Al-Gburi, Z. Zakaria, I. M. Ibrahim, and E. B. A. Halim, "Microstrip patch antenna arrays design for 5G wireless backhaul application at 3.5 GHz," *Recent Advances in Electrical and Electronic Engineering and Computer Science: Selected articles from ICCEE 2021*, 2022, pp. 77–88.
[30] M. F. Zambak *et al.*, "A compact 2.4 GHz L-shaped microstrip patch antenna for ISM-band internet of things (IoT) applications," *Electronics (Switzerland)*, vol. 12, no. 9, p. 2149, May 2023, doi: 10.3390/electronics12092149.

BIOGRAPHIES OF AUTHORS

Magnoudewa Alaba is currently pursuing a Master's degree as a research student at the Pan African University, specifically at the Institute for Basic Sciences, Technology, and Innovation (PAUSTI) in Kenya. Her academic journey began with the attainment of a Bachelor of Science (BSc) degree in Electronics Engineering, specializing in Telecommunication Networks. She earned this degree from Ghana Telecom University College, situated on Nsawam Rd in Accra, Ghana. Her research interests span across various areas, including the design of RF and microwave components, communication systems, and the exploration of emerging wireless communication standards. She can be contacted at email: alaba.magnoudewa@students.jkuat.ac.ke.

Prof. Dominic Bernard Onyango Konditi is a faculty member in the Electrical and Electronic Engineering Department at the Technical University of Kenya (TU-K). He earned his doctoral degree in Electronics and Computer Engineering from IIT Roorkee, India, and holds an M.Sc. Engineering in Electrical and Communication Engineering from Tottori University, Japan. Additionally, he completed a postdoctoral research program at Dresden University of Technology (DUT), Germany. The professor's primary research interests revolve around the design and modeling of smart antennas, analysis and modeling of radio wave propagation, and addressing electromagnetic compatibility and electromagnetic interference issues. He has extensive experience teaching and supervising students at the postgraduate level and has contributed significantly to reputable journals and conference proceedings through his publications. He can be contacted at email: dominic.konditi@tukenya.ac.ke.

Prof. Vitalice Kalecha Oduol completed his pre-university education at Alliance High School in Kenya. Subsequently, he pursued his academic journey at McGill University in Montréal, Canada, where he obtained his B.Eng. (Hons.), M.Eng., and Ph.D. degrees in Electrical Engineering in 1985, 1987, and 1992, respectively. Following that, he joined MPB Technologies, Inc. from 1998 to 2002, where he contributed to communication systems product definition and architecture. His research focuses on various aspects of communication systems, including performance analysis, modeling, simulation, and evaluation. This encompasses signal processing, spectrum sensing in cognitive radio, emerging areas such as 5G and beyond, and mitigating rain attenuation in RF signals at high frequencies. Notably, he is a member of IEEE and was honored with the Douglas Tutorial Scholarship at McGill University on two occasions. He can be contacted at email: vitalice.oduol@gmail.com.